

A Rigid Harness with Haptic Feedback for Robotic and Traditional Service Dogs

Amalie J. Keefe¹, Justin Kauff¹, and Blake Hament^{1*}.

*bhament@elon.edu

¹ Department of Engineering
Elon University
Elon, United States

Abstract—This project aims to develop a harness for the Unitree Go1 and Go2 quadrupeds that implements haptic feedback to the user when obstacles are encountered in their path. This research builds upon previous robotic Seeing Eye dog designs, incorporating feedback from a focus group session, which has led to further understanding what some members of the visually impaired community value in assistive devices. Though future implementations of this work may include more advanced object detection, with computer vision tools such as LiDAR, this project uses an Arduino Uno and ultrasonic sensors for proof of concept. The final deliverable of this project is a functional prototype implemented on the robotic quadruped that includes vibration motors, adaptable mechanical integration, and an ergonomic handle for the harness. Technical design requirements have been outlined, including battery life, budget, and handle dimensions and weight. The prototype will be reviewed at an additional upcoming focus group session for feedback and iterative design. Incorporating user responses to make a useful and desired product, this research looks to advance equity, inclusion, and accessibility for members of the visually impaired community, aiding their independence through ease of navigation in unfamiliar spaces.

Keywords—assistive robotics, robotic service dog, rigid harness, haptic vibration feedback.

I. INTRODUCTION

Seeing Eye dogs are important aides for many members of the visually impaired community. Yet for some individuals, having a live service animal is an extreme burden in terms of cost, care, and more. A robotic alternative could better suit the needs of some users, with less maintenance, greater longevity, and increased individualization. This research aims to explore the development of robotic service dogs (RSD) for people with visual impairments. A traditional rigid harness was adapted with vibration motors, creating a familiar feeling tool with a new type feedback. This prototype is demonstrated in Figure 1. This type of vibration feedback could also be implemented on a traditional, live Seeing Eye dog with a rigid harness as shown in Figure 2.

II. LITERATURE REVIEW

Haptic feedback has significant usages both outside of robotics and within it [1]–[7]. The most popular applications are with smartphones, gaming applications, and virtual reality systems [3], [8]–[10]. More recently, haptic vibration has been involved in medical robotics to give surgeons feedback



Fig. 1. A Unitree Go1 quadruped was equipped with the rigid harness device.

when conducting robotically assisted operations [6], [10]–[12]. There has also been research into using haptic feedback as a way to assist individuals with difficulty processing sensory information [7]. Thus, the understanding of haptic vibration feedback is ever growing for usages that range from medical, to recreational, to daily life.

Haptic vibration feedback has significant research to aid in adapting service technologies for individuals with visual disabilities [13]–[18]. There are several methods of implementing haptic feedback. One popular method is through wearable technology such as bracelets, gloves, or belts [13], [17], [18]. The placement of the device varies with what method of sensing is used. When using something attached to the wrists or hands of the user, there is more movement to try to account



Fig. 2. Traditional, live Seeing Eye dogs use rigid harnesses of a similar style to the proposed device.

for with a typical human gait than mounting close to the user’s center of mass [13], [18]. Thus some researchers attempt to place sensors in places with more predictable and limited movement, such as integrating with glasses [13]. Often, these projects force the individual to learn totally new technologies and systems, rather than updating familiar technology.

Finally, this research builds off of past focus group session feedback [19], [20]. This includes creating a RSD AI voice module for a Go1 quadruped and developing a “smart” cane with LiDAR detection [19], [20]. This variation allows for individuals to select their own preference rather than hyper-focusing on one type of assistive device.

III. SYSTEM DESIGN

The Unitree Go1 was used as the platform for this iteration of RSD device. A base plate was modeled in SolidWorks and 3D printed to connect to the back plate of the dog. This base plate allows for connection to the 5 step articulating hinges as well as the electronics box. The hinges allow for customization of the angle of the rigid harness. This allows the user to adjust the handle height and the horizontal distance to the quadruped. The electronics housing box contains all the necessary sensors and controls. The motors are mounted in the handle of the rigid harness. The physical prototype is shown in Figure 3.

The system was designed to provide distance-dependent haptic feedback using ultrasonic sensing and DC motor actuation. Three ultrasonic sensors were used to detect the proximity of objects, and each sensor was paired with a corresponding DC motor. The intensity of motor vibration was modulated based on the measured distance, such that closer objects produced stronger vibrations. This system focuses on close-range obstacle avoidance. The furthest distance to alert the user is 75 cm, and the closest is 3 cm.

The system was implemented using an Arduino UNO R4 microcontroller, 2 dual H-bridge motor drivers, and DC motors. Distance measurements are continuously acquired, processed, and mapped to motor control signals in real time.

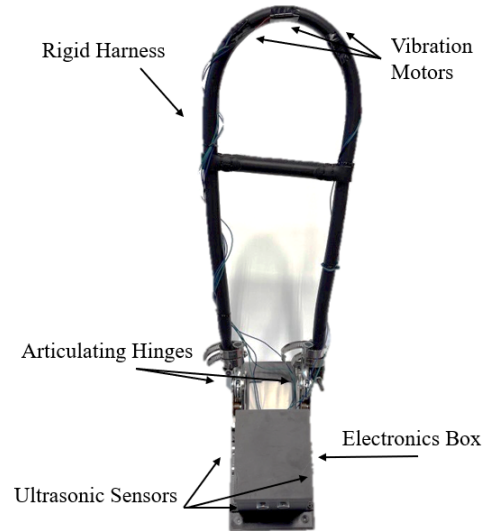


Fig. 3. The haptic feedback harness delivers vibrational feedback to the user’s hand.

A. Hardware Configuration

Each ultrasonic sensor was connected to the Arduino using a trigger (TRIG) and echo (ECHO) pin pair. The sensors operate by emitting an ultrasonic pulse and measuring the time required for the reflected signal to return, enabling distance calculation based on the speed of sound. The three DC motors were controlled using two motor driver modules. Each motor driver channel consisted of two digital input pins for direction control, and one enable pin for speed control via pulse-width modulation (PWM). The enable pins were connected to PWM-capable pins on the Arduino to allow continuous variation in motor speed. An external battery pack was used to power the motors. All system components shared a common ground to guarantee consistent signal referencing and reliable operation. This can be seen in a simplified schematic in Figure 4.

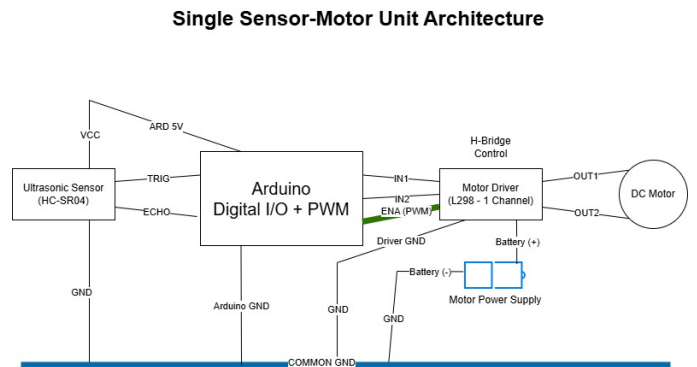


Fig. 4. A simplified schematic of a single sensor–motor unit is shown above. The ultrasonic sensor provides distance measurements to the microcontroller, which generates PWM signals to control motor speed through a motor driver. The motor is powered by an external supply, and all components share a common ground.

B. Distance Measurement

Distance measurements were obtained using a time-of-flight approach. For each sensor, the Arduino generated a 10 μ s pulse on the trigger pin, causing the sensor to emit an ultrasonic wave. The duration of the returning echo pulse was measured using the pulseIn() function. This duration was converted to distance using:

$$d = \frac{t * v}{2} \quad (1)$$

Where t is the measured echo time and v is the speed of sound in air 0.0343cm μ s. The division by two accounts for the round-trip travel of the signal. To reduce interference between sensors, measurements were taken sequentially with short delays between each reading.

C. Motor Control Strategy

Each motor was controlled independently using a unidirectional drive scheme. Direction pins were set to maintain forward rotation, while speed was controlled through PWM signals applied to the enable pins of the motor drivers. The Arduino's analogWrite() function was used to generate PWM signals with values ranging from 0 to 255, corresponding to 0% to 100% duty cycle. A value of zero resulted in no motor activity, while higher values increased the average voltage supplied to the motor, producing stronger vibration.

D. Distance to Speed Mapping

A mapping function was implemented to convert measured distance into a motor speed command. Two threshold parameters were defined: a minimum detection distance and a maximum detection distance. Distances greater than the maximum threshold resulted in the motor being turned off, while distances below the minimum threshold produced maximum motor speed.

For distances within this range, a normalized "closeness" value was computed and mapped to a PWM output range. To enhance perceptual sensitivity, a nonlinear scaling function was applied to the normalized distance, emphasizing stronger changes in motor output at closer distances. This approach improved the responsiveness of the system and made variations in proximity more perceptible to the user. Additionally, a minimum active motor speed was enforced to overcome the dead zone of the motors, ensuring that once activated, each motor produced a noticeable vibration.

E. Software Implementation

The control logic was implemented in the Arduino IDE using a modular structure. Separate functions were defined for distance measurement, distance-to-speed conversion, and motor actuation. This modular design improved code readability and allowed for easier parameter tuning. Within the main loop, the system continuously:

- 1) Measured distances from each ultrasonic sensor
- 2) Converted each distance measurement into a corresponding motor speed
- 3) Updated each motor's PWM signal accordingly

- 4) Output diagnostic data to the serial monitor for debugging and calibration

Delays were introduced between sensor readings and loop iterations to reduce signal interference and ensure stable operation.

Algorithm 1 Main Control Loop

```

1: Initialize sensor and motor pins
2: Stop all three motors
3: while system is running and repeat for each motor do
4:    $d_n \leftarrow \text{MeasureDistance}(\text{sensor}_n)$ 
5:   wait(sensor delay)
6:    $s_n \leftarrow \text{ConvertDistanceToSpeed}(d_n)$ 
7:   DriveMotor(motor $_n$ ,  $s_n$ )
8:   Output diagnostic data
9:   wait(loop delay)
10: end while=0

```

Algorithm 2 MeasureDistance

Require: triggerPin, echoPin

Ensure: distance (cm)

```

1: Set triggerPin LOW
2: wait(2 microseconds)
3: Set triggerPin HIGH
4: wait(10 microseconds)
5: Set triggerPin LOW
6:  $\text{echoDuration} \leftarrow \text{MeasurePulseDuration}(\text{echoPin})$ 
7: if  $\text{echoDuration}$  is invalid then
8:   return -1
9: end if
10:  $\text{distance} \leftarrow \frac{\text{echoDuration} \times \text{speed\_of\_sound}}{2}$ 
11: return distance =0

```

Algorithm 3 ConvertDistanceToSpeed

Require: distance (cm)

Ensure: motorSpeed (PWM value)

```

1: if distance  $\leq$  0 then
2:   return 0
3: end if
4: if distance  $\geq$  MAX_DISTANCE then
5:   return 0
6: end if
7: if distance  $\leq$  MIN_DISTANCE then
8:   return MAX_SPEED
9: end if
10:  $\text{closeness} \leftarrow \frac{\text{MAX\_DISTANCE} - \text{distance}}{\text{MAX\_DISTANCE} - \text{MIN\_DISTANCE}}$ 
11:  $\text{adjustedCloseness} \leftarrow \text{closeness}^2$ 
12:  $\text{motorSpeed} \leftarrow \text{MIN\_ACTIVE\_SPEED} +$   

   ( $\text{MAX\_SPEED} - \text{MIN\_ACTIVE\_SPEED}$ )  $\times$   

    $\text{adjustedCloseness}$ 
13: Clamp(motorSpeed, valid range)
14: return motorSpeed =0

```

IV. METHODOLOGY

There were two main testing objectives at this stage of development in the prototype. In the first test, the ultrasonic sensors were sampled at set distances to observe the sensor noise. First, a target object was placed at the far edge of the sensor range (118 cm away) and sensor values were collected over a set time frame of 14 seconds. For the second test, an obstacle was moved between various pre-measured distances for 4-6 seconds per setpoint. The distances were 3 cm, 22 cm, 48 cm, and 58 cm. Again, the distance sensed was recorded in terms of time. For these two tests, a statistical outlier filter was applied by finding standard deviation as shown:

$$\sigma = \sqrt{\frac{\sum(x - \bar{x})^2}{n - 1}} \quad (2)$$

where x is the sample, \bar{x} is sample mean, and n is the sample size. Points outside of the standard deviation were filtered out. Finally, a third test was conducted in which the frequency of vibration was varied with the distance of obstacle detection as described in Algorithm 3. To test this, the system was placed on the robotic quadruped and motor vibration speed was read at various distances from the obstacle.

V. RESULTS

Figure 5 demonstrates the effect of having the obstacle 118 cm away from the system. This graph demonstrates some sensor noise, though it was minimal and stabilized after 10 seconds stationary pose. However, without filtering, this would cause some sensor vibration from false obstacle detections. After applying the statistical outlier filter, the noise significantly decreased as shown in Figure 6. There is still some noise, but nothing that would trigger the vibration motors into a false readout unlike the outliers from Figure 5. Still, other methods of further eliminating false readings should be used, like incorporating a moving average or slightly increasing the amount of time between sensor readouts to minimize the likelihood that false values are reported.

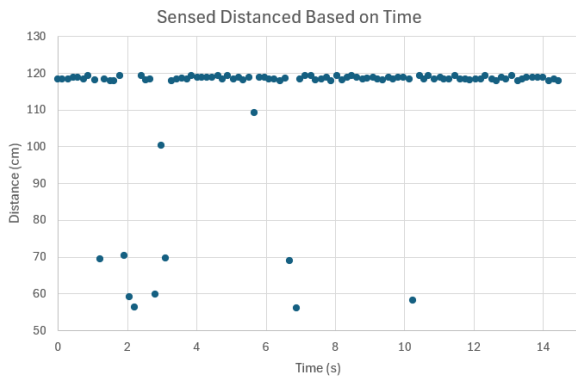


Fig. 5. Sensor readouts at 118 cm show noise prior to performing statistical outlier removal.

Figure 7 demonstrates the sensor readout for a target moving relative to the RSD. As depicted, under 50 cm, there is minimal

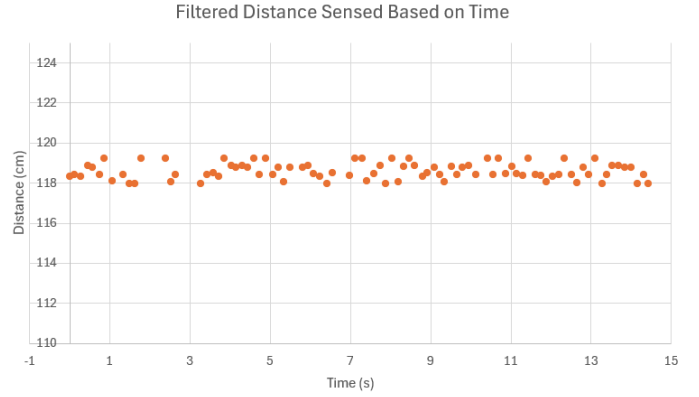


Fig. 6. Sensor readouts at 118 cm after performing statistical outlier removal show massive noise reduction.

error with the sensor readouts. The closer the object is, the more accurate the sensor is. However, at 58 cm, there are more false readouts in the data. However, all the distances detected at that time were within the detection range, which means that the sensor did not stop vibrating. This demonstrates that even with some noise around 60 cm away from the system, the user would experience slight fluctuation in vibration feedback, but still be alerted the entire time. After performing statistical outlier analysis, Figure 8 shows minimal noise. Both Figure 7 and 8 alerted the user continuously of objects in their path.

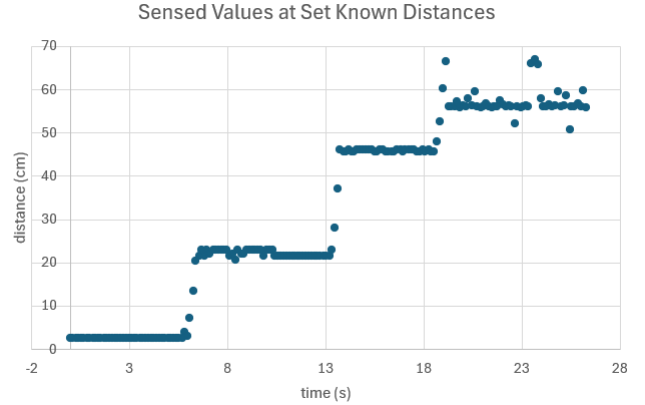


Fig. 7. Sensor readouts for the varied distances test before performing statistical removal shows significant noise at obstacle distance of 58 cm.

Finally, Figure 9 shows how the frequency of vibration increases as the object gets closer to the user. The test explored distances from 3 cm to 75 cm between the obstacle and the prototype. What little sensor noise remains after filtering is largely smoothed out when the distance is converted to haptic feedback as a vibration frequency signal.

VI. CONCLUSIONS

The next step for this research is to conduct another focus group session and to receive feedback from members of the visually impaired community on this device. This focus group

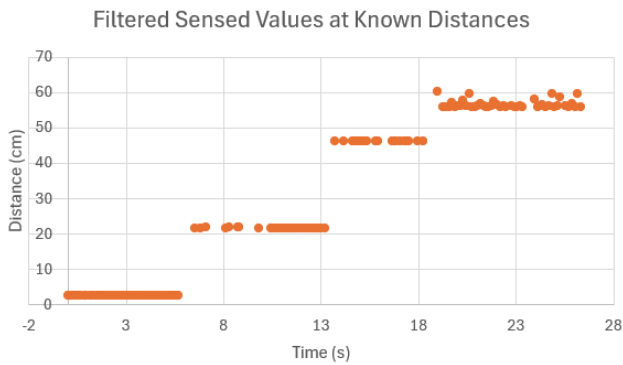


Fig. 8. Sensor readouts for the varied distances test after performing statistical outlier filtering reduced the sensor noise.

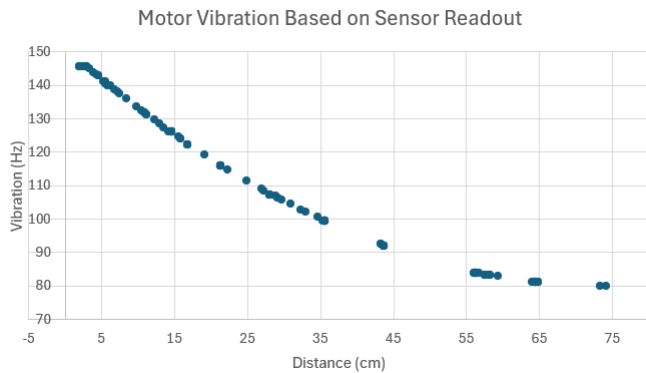


Fig. 9. Vibration frequency is mapped from the sensed obstacle distance to give users higher frequency haptic feedback for obstacles that are close and lower frequency haptic feedback for obstacles that are further away.

will allow for interaction with the prototype developed and a group Q&A session and discussion. This will allow for a better understanding of how future work can best support individuals and enhance their comfort when using such a device.

Additional testing will also be conducted prior to the focus group including testing the 2D feedback field, identifying coordinates of objects in the sensor field, and scaling haptic response of the different motors to give a better sense of obstacles in 2D. This testing will elevate the quality of the prototype that will be presented to the focus group, allowing for a better understanding of what changes should be implemented. Further testing should include leading a member of the research team through an obstacle course based on the feedback detected.

This research shows the significant work done in adapting a rigid harness to return haptic vibration feedback to a user with visual impairments with the ability for individual customization. Yet, there is more work to be done to ensure a safe and well tested mechanism.

ACKNOWLEDGMENT

Thank you to both the Elon University Maker Hub Kickbox program and Elon University's Research Grant-in-Aid grant

for funding this project. Additional thanks to William Corkey for spending significant time discussing ideas with me and providing feedback.

REFERENCES

- [1] H. W. Tappeiner, R. L. Klatzky, B. Unger, and R. Hollis, "Good vibrations: Asymmetric vibrations for directional haptic cues," in *World Haptics 2009 - Third Joint EuroHaptics conference and Symposium on Haptic Interfaces for Virtual Environment and Teleoperator Systems*, 2009, pp. 285–289.
- [2] J. R. Blum, I. Frissen, and J. R. Cooperstock, "Improving haptic feedback on wearable devices through accelerometer measurements," in *Proceedings of the 28th Annual ACM Symposium on User Interface Software and Technology (UIST '15)*. New York, NY, USA: Association for Computing Machinery, 2015, pp. 31–36. [Online]. Available: <https://doi.org/10.1145/2807442.2807474>
- [3] X. Tang, A. Talhan, H. Nisar, R. Lindgren, and M. Lira, "Good vibrations: Feeling and interpreting haptic feedback," in *Proceedings of the 19th International Conference of the Learning Sciences (ICLS 2025)*. International Society of the Learning Sciences (ISLS), 2025. [Online]. Available: <https://doi.org/10.22318/icls2025.360851>
- [4] A. Chang and C. O'Sullivan, "Audio-haptic feedback in mobile phones," in *CHI '05 Extended Abstracts on Human Factors in Computing Systems*, ser. CHI EA '05. New York, NY, USA: Association for Computing Machinery, 2005, p. 1264–1267. [Online]. Available: <https://doi.org/10.1145/1056808.1056892>
- [5] W. H. Hampton and C. Hildebrand, "Haptic rewards: How mobile vibrations shape reward response and consumer choice," *Journal of Consumer Research*, vol. 52, no. 5, pp. 1043–1070, 2026. [Online]. Available: <https://doi.org/10.1093/jcr/ucaf025>
- [6] J. O'Neill, D. A. O'Neill, W. J. Lewinski, and M. E. Hartman, "Toward a taxonomy of the unintentional discharge of firearms in law enforcement," *Applied Ergonomics*, vol. 59, pp. 283–292, 2017. [Online]. Available: <https://www.sciencedirect.com/science/article/pii/S0003687016301661>
- [7] K. Krishnan, N. Jomhari, R. Kumar Ayyasamy, S. Abdul Kareem, and S. Krishnan, "Haptic feedback: An experimental evaluation of vibrations as tactile sense in autistic people," *IEEE Access*, vol. 12, pp. 81 088–81 104, 2024.
- [8] R. Nayak, S. Mishra, P. Rane, P. Narayan, and N. Prabhu, "Development of a wearable haptic guidance system for visually impaired using gps and vibration feedback," *Applied Sciences*, vol. 12, no. 9, p. 4686, 2022. [Online]. Available: <https://doi.org/10.3390/app12094686>
- [9] C.-M. Wu, C.-W. Hsu, T.-K. Lee, and S. Smith, "A virtual reality keyboard with realistic haptic feedback in a fully immersive virtual environment," *Virtual Reality*, vol. 21, no. 1, pp. 19–29, 2017. [Online]. Available: <https://doi.org/10.1007/s10055-016-0296-6>
- [10] K. Bark, W. McMahan, A. Remington, J. Gewirtz, A. Wedmid, D. I. Lee, and K. J. Kuchenbecker, "In vivo validation of a system for haptic feedback of tool vibrations in robotic surgery," *Surgical Endoscopy*, vol. 27, no. 2, pp. 656–664, February 2013. [Online]. Available: <https://doi.org/10.1007/s00464-012-2452-8>
- [11] C. Pacchierotti, D. Prattichizzo, and K. J. Kuchenbecker, "Cutaneous feedback of fingertip deformation and vibration for palpation in robotic surgery," *IEEE Transactions on Biomedical Engineering*, vol. 63, no. 2, pp. 278–287, 2016.
- [12] I. El Rassi and J.-M. El Rassi, "A review of haptic feedback in tele-operated robotic surgery," *Journal of Medical Engineering & Technology*, vol. 44, no. 5, pp. 247–254, July 2020. [Online]. Available: <https://doi.org/10.1080/03091902.2020.1772391>
- [13] S. Scheggi, A. Talarico, and D. Prattichizzo, "A remote guidance system for blind and visually impaired people via vibrotactile haptic feedback," in *22nd Mediterranean Conference on Control and Automation*, 2014, pp. 20–23.
- [14] D. Kleinberg, R. Yozevitch, I. Abekasis, Y. Israel, and E. Holdengreber, "A haptic feedback system for spatial orientation in the visually impaired: A comprehensive approach," *IEEE Sensors Letters*, vol. 7, no. 9, pp. 1–4, 2023.
- [15] S. Khusro, B. Shah, I. Khan, and S. Rahman, "Haptic feedback to assist blind people in indoor environment using vibration patterns," *Sensors*, vol. 22, no. 1, p. 361, January 2022. [Online]. Available: <https://doi.org/10.3390/s22010361>
- [16] S. Kammoun, C. Jouffrais, T. Guerreiro, H. Nicolau, and J. Jorge, "Guiding blind people with haptic feedback," 01 2012.

- [17] R. K. Katzschmann, B. Araki, and D. Rus, "Safe local navigation for visually impaired users with a time-of-flight and haptic feedback device," *IEEE Transactions on Neural Systems and Rehabilitation Engineering*, vol. 26, no. 3, pp. 583–593, 2018.
- [18] S. T. H. Rizvi, M. J. Asif, and H. Ashfaq, "Visual impairment aid using haptic and sound feedback," in *2017 International Conference on Communication, Computing and Digital Systems (C-CODE)*, 2017, pp. 175–178.
- [19] A. J. Keefe and B. Hament, "Artificial intelligence (ai) voice module for robotic service dog," *2024 Systems and Information Engineering Design Symposium (SIEDS)*, pp. 296–300, 2024. [Online]. Available: <https://api.semanticscholar.org/CorpusID:269953964>
- [20] M. Dion and B. Hament, "Designing an interactive cane for the visually impaired," *2025 Systems and Information Engineering Design Symposium (SIEDS)*, pp. 173–178, 2025. [Online]. Available: <https://api.semanticscholar.org/CorpusID:279172297>